



A Statistical Survey of Low-Frequency Magnetic Fluctuations at Saturn

Dong-Xiao Pan¹, Zhong-Hua Yao¹, Rui-Long Guo², Bertrand Bonfond², Yong Wei¹, William Dunn³, Bin-Zheng Zhang⁴, Qiu-Gang Zong⁵, Xu-Zhi Zhou⁵, Denis Grodent², and Wei-Xing Wan¹

¹Key Laboratory of Earth and Planetary Physics, Institute of Geology and Geophysics, Chinese Academy of Sciences, Beijing, China

²Laboratoire de Physique Atmospherique et Planetaire, STAR institute, Universite de Liege, Liege, Belgium

³University College London, Mullard Space Science Laboratory, Dorking, UK

⁴Department of Earth Sciences, the University of Hong Kong, Hong Kong SAR, China

⁵School of Earth and Space Sciences, Peking University, Beijing, China

Key Points:

- Using the complete Cassini magnetometer dataset, we present the global picture of ULF waves in Saturn's magnetosphere.
- The wave power shows a rapid decrease beyond 25 R_S in both the morning and afternoon sectors.
- The wave activity peaks in noon sector, implying that these waves could be driven by the solar wind interaction with Saturn's magnetopause.

Corresponding author: Zhong-Hua Yao, z.yao@ucl.ac.uk

This article has been accepted for publication and undergone full peer review but has not been through the copyediting, typesetting, pagination and proofreading process, which may lead to differences between this version and the [Version of Record](#). Please cite this article as doi: [10.1029/2020JA028387](https://doi.org/10.1029/2020JA028387).

This article is protected by copyright. All rights reserved.

Abstract

Low-frequency waves are closely related to magnetospheric energy dissipation processes. The Cassini spacecraft explored Saturn's magnetosphere for over 13 years, until September 2017, covering a period of more than a complete solar cycle. Using this rich heritage dataset, we systematically investigated key physical parameters of low-frequency waves in Saturn's magnetosphere, including their local time distribution and the dependence on solar activity. We found that the wave activity peaked in the near noon sector. For the nightside, the wave intensity also appeared to peak pre and post-midnight. Due to the limited local time coverage for each solar phase, we were not able to draw a firm conclusion on the waves dependence on solar activity. In general, the wave power showed a monotonically decreasing trend towards larger distances in nightside sectors especially during the declining phase, which implied that low-frequency waves mainly originate from the relatively inner regions of the magnetosphere. On the dayside, stronger waves were mostly located at/within $\sim 25 R_s$, near the magnetopause. The study shows a global picture of low-frequency waves in Saturn's magnetosphere, providing important implications for how magnetospheric energy dissipates into Saturn's polar ionosphere and atmosphere.

1 Introduction

For the terrestrial magnetosphere the plasma source is predominately the solar wind via the Dungey cycle process (Dungey, 1961). In contrast, the particle source for Saturn's outer magnetosphere is escaping water vapor from its moon Enceladus (Hansen et al., 2006; Waite et al., 2006; Blanc et al., 2015), which drives Saturn's magnetospheric processes. Despite different energy sources at each planet, similarities are found in many fundamental processes. For example, magnetic reconnection and dipolarization processes are fundamental plasma processes in accelerating and circulating particles in the magnetosphere, and they are found at Earth (Baker et al., 1996; Angelopoulos et al., 2008; Akasofu, 2017), Mercury (Slavin et al., 2009; Sun et al., 2015), Saturn (Jackman et al., 2007, 2015; Yao et al., 2017a) and Jupiter (Russell et al., 1998; Vogt et al., 2010; Yao et al., 2019). Recent studies also reveal similar auroral structures between Saturn and Earth (Radioti et al., 2017; Yao et al., 2017b; Radioti et al., 2019), due to the similar processes.

Among the similarities between planetary magnetospheric processes, low-frequency plasma waves, also known as ultralow frequency (ULF) waves (Hasegawa & Chen, 1974; Lee & Lysak, 1989; Chen, 1999; Zong et al., 2009), have been extensively investigated at different planets (Glassmeier et al., 2004; Kleindienst et al., 2009), as they are fundamental perturbations in magnetized plasma environments. Due to the very different sizes of planetary magnetospheres, the eigenfrequency of magnetic field line resonances between the northern and southern hemispheres can vary significantly from planet to planet. For example, the fundamental periods of magnetic field line resonances at Earth are usually a few minutes, while the fundamental periods for Mercury are a few seconds and for the giant planets they can be tens of minutes (Glassmeier et al., 2004; Kleindienst et al., 2009). Despite the large difference in temporal scales, the fundamental physical processes are similar.

The low-frequency waves at Saturn are generated by various processes. Kelvin-Helmholtz vortices, a consequence of solar wind-magnetosphere interaction, are often formed on Saturn's dawnside magnetopause, which could systematically excite field line resonances (Masters et al., 2009, 2010; Delamere et al., 2013). The plasma circulation from Vasyliunas (internally driven) reconnection may also be an energy source to excite magnetic field line resonances (Yao et al., 2017c). Furthermore, solar wind compressions could also directly form compressional mode waves on the magnetopause, and the wave would transform into shear Alfvén waves when propagating towards the inner magnetosphere (Zong et al., 2017; Allan & Poulter, 1992). To date, it is unclear whether or not there is a system-

71 atic correlation between solar activity and Saturns low-frequency wave activities. In this
 72 study, the low-frequency waves at Saturn are defined as magnetic perturbations at pe-
 73 riods of 10-60min.

74 The low-frequency fluctuations have been identified not only from magnetic field
 75 measurements, but also from aurora and energetic particle observations, indicating that
 76 these fluctuations are global processes from the magnetosphere to the ionosphere and
 77 atmosphere. Quasi-periodic 1-hour pulsations are found at Saturns cusp aurora (Palmaerts,
 78 Radioti, et al., 2016). Such pulsations are believed to be connected to in situ observa-
 79 tions of particle pulsations in the magnetosphere, which have similar periodicities (Palmaerts,
 80 Roussos, et al., 2016; Roussos et al., 2016). The Kelvin-Helmholtz instability is often con-
 81 sidered to be a plausible mechanism for these pulsations. A recent study suggests that
 82 rotationally driven magnetodisc reconnection could also trigger such pulsations (Guo,
 83 Yao, Wei, et al., 2018), although the detailed connections are yet to be understood.

84 Throughout its mission, the Cassini spacecraft collected in situ magnetic field data
 85 from Saturn throughout an entire solar cycle. The large dataset allows us to perform a
 86 systematic investigation of Saturns low-frequency magnetic fluctuations, including lo-
 87 cal time distributions and the dependence on solar activity. In this paper, we perform
 88 a statistical survey of low-frequency magnetic perturbations (with periods between 10-
 89 60min) using the large Cassini magnetometer (MAG) dataset (Dougherty et al., 2004).

90 **2 Cassini Observations From 2005 to 2014: Dependence on Solar Ac-** 91 **tivity**

92 We investigate low-frequency magnetic fluctuations at Saturn from 2005 to 2014.
 93 Based on the 27-day averaged sunspot number adopted from the omni dataset (Figure
 94 1a), we further select four subsets from the Cassini MAG observations to represent dif-
 95 ferent solar cycle phases. Each subset includes measurements during a two-year explo-
 96 ration, i.e., during the declining phase (2005-2006), solar minimum (2008-2009), ascend-
 97 ing phase (2010-2011), and solar maximum (2013-2014), respectively. Figure 1b-1i present
 98 Cassini trajectories for the four subsets in Kronocentric Solar Magnetospheric (KSM)
 99 system. During the selected 8 years, Cassinis trajectory covered an extensive area, in-
 100 cluding all local times and with radial distance up to $\sim 65R_S$ ($1R_S = 60268\text{km}$). Nev-
 101 ertheless, we need to bear in mind that the Cassini orbits show a significant bias towards
 102 specific local times and radial distances at each solar phase, which could superpose the
 103 effects of solar activity and spatial variations.

104 To conduct the statistical analysis on low-frequency magnetic fluctuations, we ap-
 105 plied the Lomb-Scargle periodogram method (Lomb, 1976; Scargle, 1982) to obtain the
 106 power spectral density (PSD) of the fluctuating magnetic field with a 6-hour window.
 107 Figure 2 shows an example of a wave event that occurred on October 28, 2015. Figure
 108 2a and 2b present the trajectories of Cassini during this period. We used 6-hour aver-
 109 aged magnetic field measurements to represent the background magnetic field (red line
 110 in Figure 2c). Figure 2e shows the power spectrum density of the detrended magnetic
 111 field (Figure 2d). The red horizontal line is the power-level threshold that is consistent
 112 with a probability of detection of 0.99, significantly lower than the observed wave power
 113 at specific frequencies. A wave event is thus selected when the probability of detection
 114 exceeds 0.99 to ensure that the peak in the spectrum is not due to random fluctuations.
 115 For each event, we define the mean value of PSD within the periods between 10min to
 116 60min, as the wave intensity PSD_{wave} .

117 We systematically investigate Saturns low-frequency magnetic fluctuations and their
 118 dependence on solar activity. Figure 3 shows the PSD_{wave} distributions of low-frequency
 119 waves during different solar phases and strong wave (with PSD_{wave} above $10^3\text{nT}^2/\text{Hz}$)
 120 occurrence rates. The abscissa are the equatorial distances D ($D = \pm\sqrt{X_{KSM}^2 + Y_{KSM}^2}$)

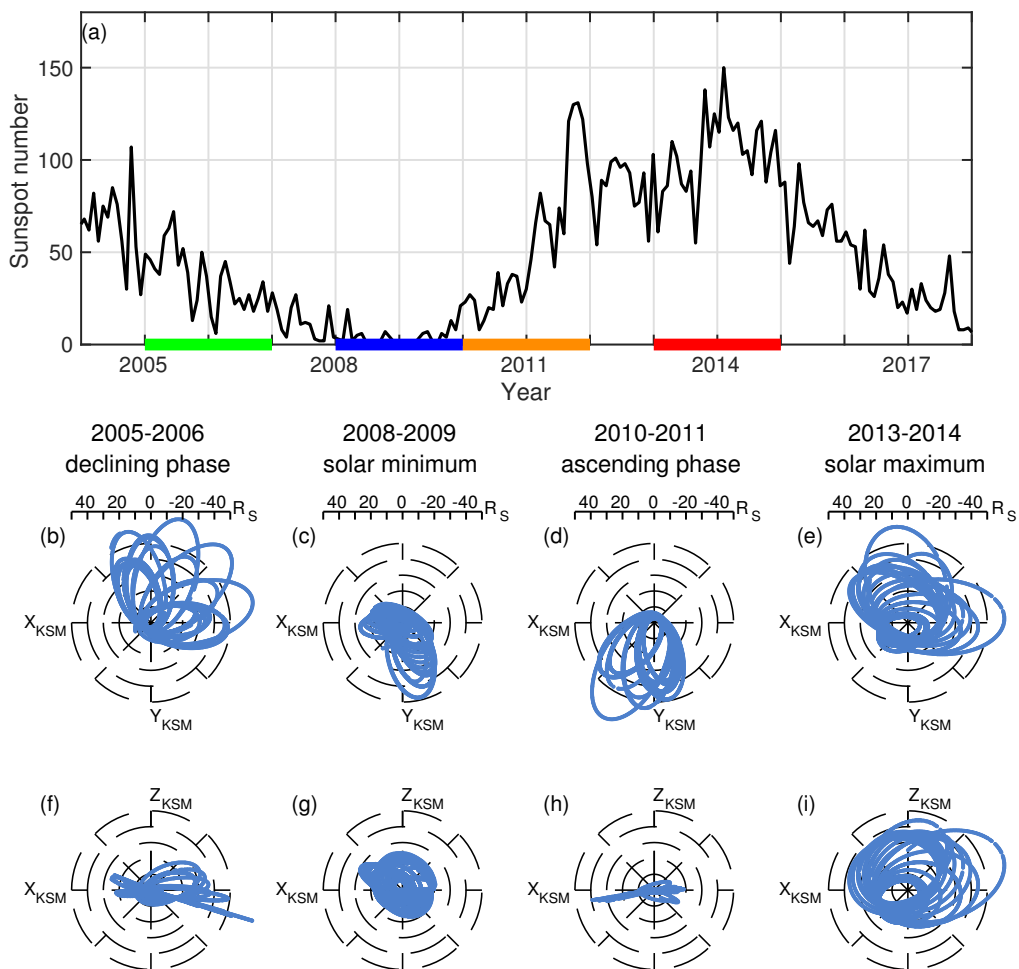


Figure 1. (a) 27-day averaged sunspot number from 2004 to 2017 adopted from omni dataset (<http://omniweb.gsfc.nasa.gov/>), the color bars mark the four solar phases; (b-i) Cassini trajectories during declining phase, solar minimum, ascending phase and solar maximum (in KSM coordinates, where X directs to the Sun, $X - Z$ plane contains Saturn's centered magnetic dipole axis and Y completes right handed set.)

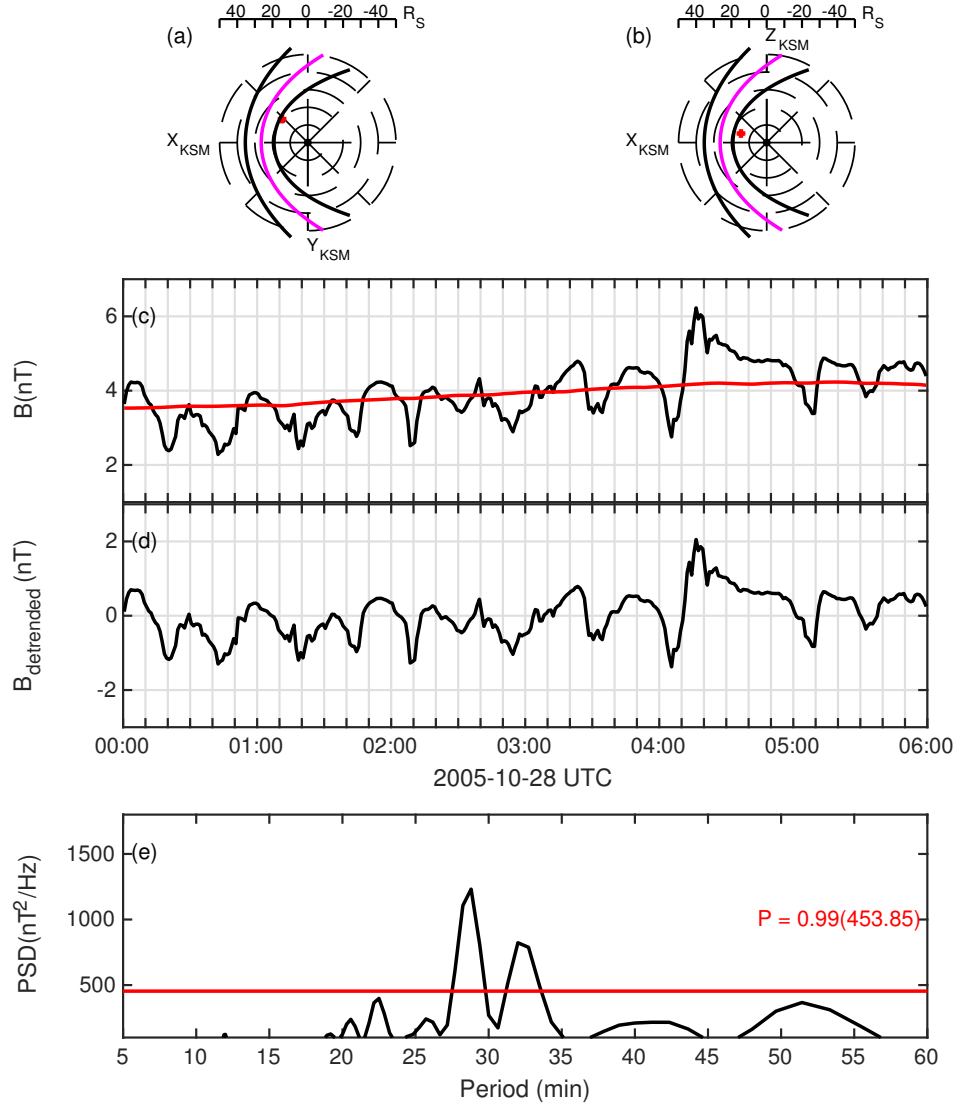


Figure 2. An example wave event on October 28, 2005. Cassini locations represented by red dots on (a) $X_{KSM} - Y_{KSM}$ and (b) $X_{KSM} - Z_{KSM}$ plane; The magenta and black curves are potential and possible magnetopause positions based on the A06 model with improved parameters for solar wind pressure of 0.00906Pa (Kanani et al., 2010; Guo, Yao, Wei, et al., 2018)(c) The intensity of the magnetic field detected by Cassini MAG instrument. The red curve represents background magnetic field, obtained from 6-hour running average. (d) The detrended magnetic field and (e) power spectral density (PSD) for the detrended magnetic field which is obtained from the Lomb-Scargle periodogram method. The red horizontal line shows power-level thresholds that are consistent with a probability of detection equal to 0.99.

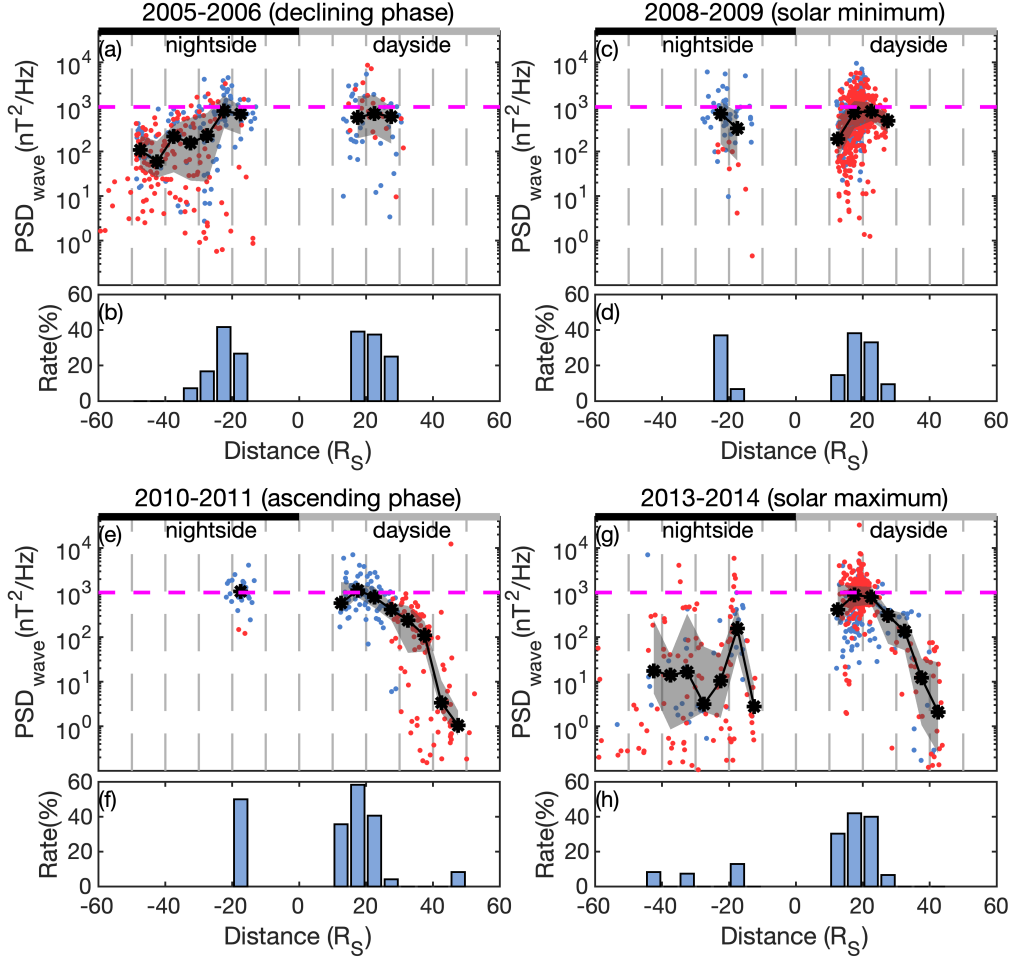


Figure 3. Scatterplots of low-frequency waves PSD_{wave} versus equatorial distances D from Saturn (positive when $X_{KSM} > 0$; negative when $X_{KSM} < 0$) and the occurrence rates for intense waves in different regions, during (a-b) declining phase, (c-d) solar minimum, (e-f) ascending phase and (g-h) solar maximum. The dayside sectors contain events in the local time range of 9-15 LT, while nightside events are in the local time range of 21-03 LT. Blue dots are events with $|Z_{KSM}| < 5R_S$, while red dots are events with $|Z_{KSM}| > 5R_S$. The black stars represent the median value of PSD_{wave} for each bin and the shaded areas mark events between upper quartile and lower quartile. Each bin contains at least 10 data points. Blue bar charts show occurrence rates for intense waves, which are defined as the number of events with $PSD_{wave} > 10^3 \text{ nT}^2/\text{Hz}$ divided by the number of all events in each bin.

121 from Saturn in $X_{KSM}-Y_{KSM}$ plane. The dayside wave events are selected to be those
 122 where the local time ranges from 9 to 15. The blue dots are events at low latitude with
 123 $|Z_{KSM}| < 5R_S$, and red dots are events at high latitude with $|Z_{KSM}| > 5R_S$. The
 124 black stars are the median value of PSD_{wave} for each bin, while the upper (lower) bound-
 125 aries of shaded areas are consistent with the upper (lower) quartiles, displaying the over-
 126 all trend of the data. We note that events with large PSD_{wave} ($> 10^3 \text{nT}^2/\text{Hz}$) at the
 127 dayside sector are mostly located at/within $\sim 25R_S$, indicating strong wave activities near/within
 128 magnetopause. The PSD_{wave} and the occurrence rates of these strong waves at dayside
 129 ($\sim 40\%$) are similar for the four solar cycle phases. The PSD_{wave} also shows a decreas-
 130 ing trend for $D > 30R_S$ as shown in Figures 3e and 3g. The nightside wave power spec-
 131 trum density is monotonically decreasing toward large distances during the declining phase
 132 (Figure 3a) and is largely scattered with a relatively low mean value during the solar max-
 133 imum phase (Figure 3g). There was insufficient data to obtain the trend in the night-
 134 side for the other two solar phases (Figure 3c, 3e), so that it is hard to study the day-
 135 night asymmetry or compare the nightside wave activities.

136 Figure 4 focuses on events located in the dawn sector (03-09 LT) and the dusk sec-
 137 tor (15-21 UT). The positive value of the abscissas in Figure 4 represent the dusk sec-
 138 tor ($Y_{KSM} > 0$). The wave intensity decreases with increasing equatorial distances D ,
 139 in both the dawnside (Figure 4a and 4g) and the duskside (Figure 4c and 4e) for each
 140 phase of the solar cycle. The PSD_{wave} distributions for events at high latitude (red dots)
 141 are usually much more dispersed than those events at low latitude (blue dots). We noted
 142 that the bias of the Cassini orbits strongly mixes the effects of solar activities and spa-
 143 tial variations so that it is hard to compare the dawnside/duskside wave activities. In
 144 addition, we used electron data with energy up to 28 keV provided by Cassini-CAPS (Young
 145 et al., 2004), to examine the wave intensity distribution inside the magnetopause. We
 146 analyzed the events with an electron temperature greater than 100eV, as the electron
 147 temperature in the magnetosheath is well below this value (Supplementary Figure S1
 148 and S2). The results show that only intense waves remained, implying that most of the
 149 weak waves ($PSD_{wave} < 10^3 \text{nT}^2/\text{Hz}$) are from the magnetosheath, which is consistent
 150 with the results in Figure 5 (shown later).

151 3 An Overview: Dependence on Local Time

152 In this section, we combine data from all sub-solar phases as marked in Figure 1
 153 to investigate the dependence of wave activity with spatial variations. Figure 5a and 5b
 154 shows the distribution of the wave events on the $X_{KSM}-Y_{KSM}$ and $X_{KSM}-Z_{KSM}$
 155 plane combining the data from all four subsets. Each dot represents a wave event and
 156 the color represents the wave intensity. The magenta curve predicted the magnetopause
 157 position calculated from the A06 model with improved parameters (Kanani et al., 2010)
 158 using the solar wind pressure of 0.00906Pa (Guo, et al., 2018). The inner and outer black
 159 curves represent the possible magnetopause positions corresponding to the root mean
 160 square errors of the A60 model coefficients. It is clear that the wave activity is strong
 161 near $\sim 25R_S$ and inside, especially near the subsolar point. We find that the wave activ-
 162 ity rapidly decreases outside of $\sim 25R_S$ at dayside, which is consistent with the nominal
 163 magnetopause location (Kanani et al., 2010). We would like to point out that there is
 164 little data along the subsolar line at $> 25R_S$, but the trend is clear in both the morn-
 165 ing and afternoon sectors, implying that low-frequency waves are magnetospheric as op-
 166 posed to a magnetosheath or solar wind process. The main periods of these intense waves
 167 are 30-60min, shown in Figure 5c.

168 Figure 5d shows the PSD_{wave} as a function of local time with events located at
 169 a distance D ranging from $20R_S$ to $30R_S$. The grey dots represent the wave events. The
 170 red stars are the median value of PSD_{wave} for each local time, while blue bars repre-
 171 sent the occurrence rate of intense waves. The wave activity peaks in the noon sector,
 172 implying that solar winds interaction with Saturns magnetopause is an important mech-

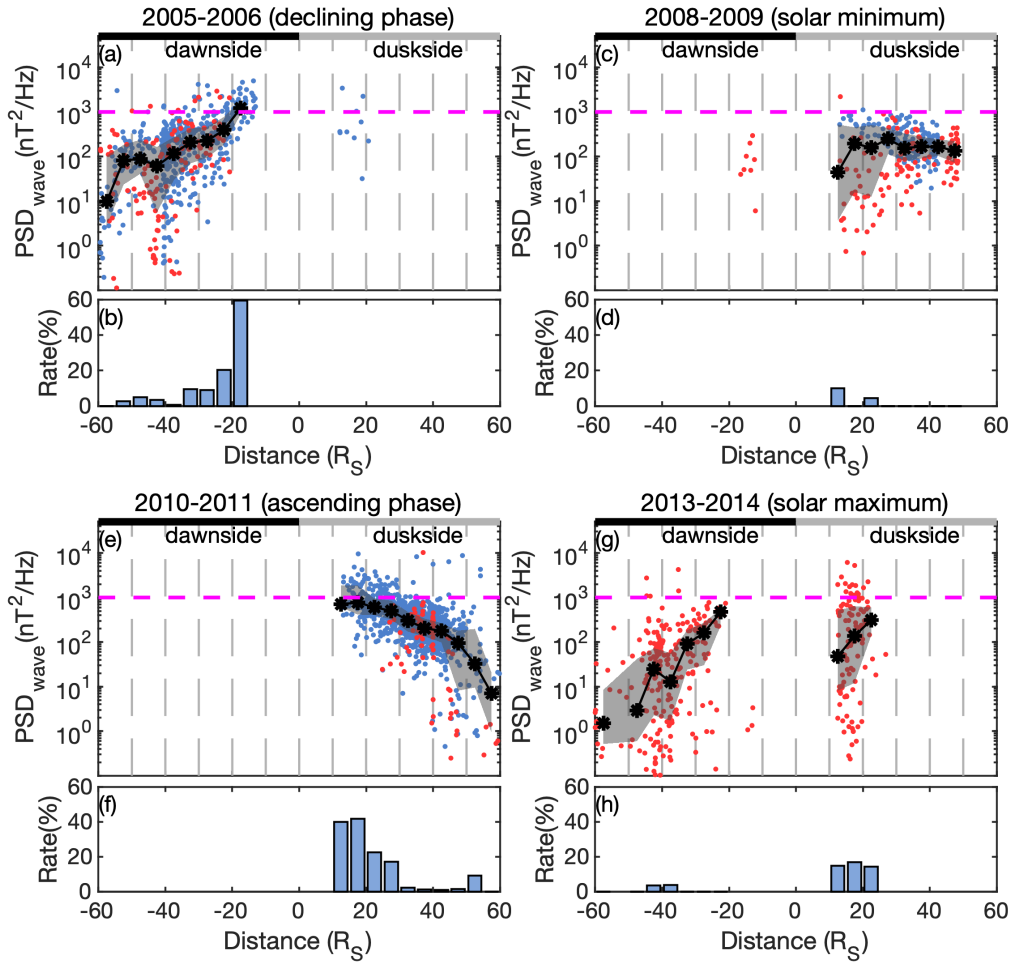


Figure 4. Same format as Figure 3, but for dawnside and duskside events. The abscissas represent equatorial distances D from Saturn (positive when $Y_{KSM} > 0$; negative when $Y_{KSM} < 0$). The dawnside sectors contain events within the range 03-09 LT, while the duskside sectors are defined as events in the local time range 15-21 LT.

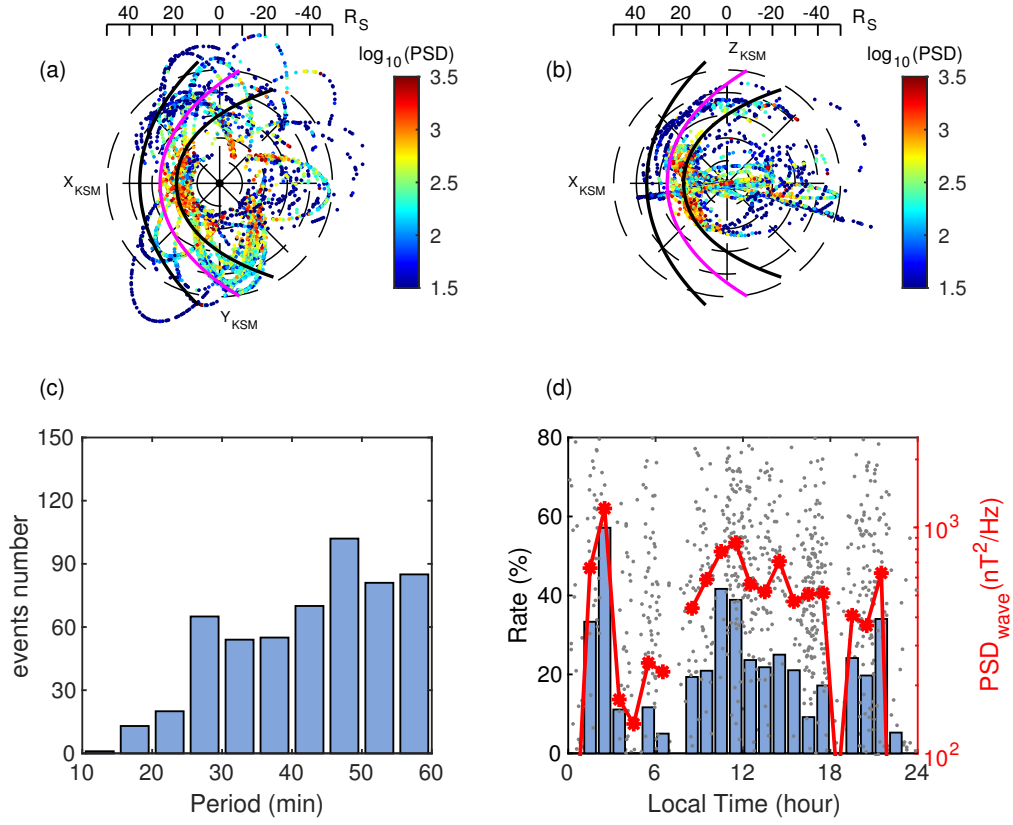


Figure 5. Low-frequency wave activity distributions on (a) $X_{KSM} - Y_{KSM}$ and (b) $X_{KSM} - Z_{KSM}$ plane. The color scheme represents the magnitude of $\log_{10}PSD_{wave}$. The magenta and black curves are potential and possible magnetopause positions based on A06 model with improved parameters for solar wind pressure of 0.00906Pa (Kanani et al., 2010; Guo, Yao, Wei, et al., 2018) (c) The distribution of periods for intense waves ($PSD_{wave} > 10^3 nT^2/Hz$) (d) The dependence of low-frequency wave power spectrum density with local time. Each grey dot represents a wave event, and red stars gives the median value of PSD_{wave} for each local time for the events located at distance D from $20R_S$ to $30R_S$. Blue bars represent the occurrence rate of intense waves for each local time.

anism in driving the magnetospheric low-frequency waves. Magnetopause surface waves (Masters et al., 2012, 2009) and/or Kelvin-Helmholtz waves (Wilson et al., 2012) caused by the interactions between the solar wind and Saturn's magnetopause are likely the major contributions. We also noted that the wave intensity also peaks at pre-midnight and post-midnight. The driver for nightside waves is inconsistent with the magnetopause surface waves. Nightside waves may instead be a consequence of Titan torus perturbation or nightside transient plasma processes (e.g., magnetic reconnection or bursty bulk flows).

4 Conclusions

Low-frequency wave activity is a consequence of many fundamental magnetospheric processes that perturb the magnetic field, energetic particles, auroral emissions, etc. In this study, the low-frequency waves are selected only based on the periodicity. There are many proposed mechanisms for driving these waves, for example, K-H instabilities or solar wind pressure pulses. Since the wave power peaks near the magnetopause, we suggest the interaction between the solar wind and the rotating magnetosphere to be pivotal for the wave generation. These waves are associated with macro-processes, thus they are likely MHD waves. However, the interaction between the solar wind and the rotating magnetosphere can also modify particle distribution and this may induce kinetic effects. The limited data coverage in local times for each solar phase does not allow us to draw a firm conclusion on a connection with solar activity. Nevertheless, no significant dependence on solar activity is identified from the existing dataset. The results also show that dayside wave activity is generally stronger than at nightside near solar maximum, probably indicating the presence of a systematic wave driver on the magnetopause. It is clear that the wave power rapidly decreases beyond $\sim 25R_S$ at morning and afternoon sectors, indicating that the detected waves are not from the magnetosheath or solar wind.

In analysing the local time sectors, we found that a peak wave power was found near the noon sector, which is probably related to the active auroral region in the prenoon sector (Bader et al., 2019). The dayside wave distribution might also be related to drizzle-like reconnection, which also displays a peak occurrence probability near noon (Delamere et al., 2015). Auroral observations suggest pulsating auroral emissions with a periodicity of ~ 60 min (Palmaerts, Radioti, et al., 2016), which is consistent with the wave periodicities shown in this study. Our results suggest that low-frequency waves could be an important source of auroral emission at Saturn, as was proposed at Earth (Keiling et al., 2003, 2019; Zhao et al., 2019) and Jupiter (Saur et al., 2018). A further study combining magnetic perturbations and auroral images will help to answer this question. It is also worth conducting a magnetohydrodynamic (MHD) simulation to examine the importance of Alfvénic precipitation in driving auroral emissions.

Acknowledgments

This work was supported by the Strategic Priority Research Program of Chinese Academy of Sciences (Grant No. XDA17010201). The Cassini data presented in this paper are available at <http://pds-ppi.igpp.ucla.edu/>. D.G. and B.B. are supported by the PRODEX program managed by ESA in collaboration with the Belgian Federal Science Policy Office. W.D. was supported by a Science and Technology Facilities Council (STFC) research grant to University College London (UCL) and by European Space Agency (ESA) contract no. 4000120752/17/NL/MH. The authors wish to thank the International Space Science Institute in Beijing (ISSI-BJ) for supporting and hosting the meetings of the International Team on 'The morphology of auroras at Earth and giant planets: characteristics and their magnetospheric implications', during which the discussions leading/contributing to this publication were held. It was also made possible by the Key Research Program of the Institute of Geology and Geophysics CAS (grant IGGCAS201904).

References

- 222
- 223 Akasofu, S.-I. (2017, OCT). Auroral substorms: Search for processes causing the
224 expansion phase in terms of the electric current approach. *Space Science Re-*
225 *views*, *212*(1-2), 341-381. doi: 10.1007/s11214-017-0363-7
- 226 Allan, W., & Poulter, E. M. (1992, May). ULF waves-their relationship to the struc-
227 ture of the Earth's magnetosphere. *Reports on Progress in Physics*, *55*(5), 533-
228 598. doi: 10.1088/0034-4885/55/5/001
- 229 Angelopoulos, V., McFadden, J. P., Larson, D., Carlson, C. W., Mende, S. B., Frey,
230 H., ... Kepko, L. (2008, AUG 15). Tail reconnection triggering substorm
231 onset. *Science*, *321*(5891), 931-935. doi: 10.1126/science.1160495
- 232 Bader, A., Badman, S. V., Cowley, S. W. H., Yao, Z. H., Ray, L. C., Kinrade, J., ...
233 Pryor, W. R. (2019, SEP 1). The dynamics of saturn's main aurorae. *Geophys-*
234 *ical Research Letters*, *46*(17-18), 10283-10294. doi: 10.1029/2019GL084620
- 235 Baker, D., Pulkkinen, T., Angelopoulos, V., Baumjohann, W., & McPherron,
236 R. (1996, JUN 1). Neutral line model of substorms: Past results and
237 present view. *Journal of Geophysical Research*, *101*(A6), 12975-13010. doi:
238 10.1029/95JA03753
- 239 Blanc, M., Andrews, D. J., Coates, A. J., Hamilton, D. C., Jackman, C. M., Jia,
240 X., ... Westlake, J. H. (2015, OCT). Saturn plasma sources and associ-
241 ated transport processes. *Space Science Reviews*, *192*(1-4), 237-283. doi:
242 10.1007/s11214-015-0172-9
- 243 Chen, L. (1999, FEB 1). Theory of plasma transport induced by low-frequency hy-
244 dromagnetic waves. *Journal of Geophysical Research*, *104*(A2), 2421-2427. doi:
245 10.1029/1998JA900051
- 246 Cutler, J. C., Dougherty, M. K., Lucek, E., & Masters, A. (2011, OCT 19). Evidence
247 of surface wave on the dusk flank of saturn's magnetopause possibly caused by
248 the kelvin-helmholtz instability. *Journal of Geophysical Research*, *116*. doi:
249 10.1029/2011JA016643
- 250 Delamere, P. A., Otto, A., Ma, X., Bagenal, F., & Wilson, R. J. (2015, JUN). Mag-
251 netic flux circulation in the rotationally driven giant magnetospheres. *Journal*
252 *of Geophysical Research*, *120*(6), 4229-4245. doi: 10.1002/2015JA021036
- 253 Delamere, P. A., Wilson, R. J., Eriksson, S., & Bagenal, F. (2013, JAN). Mag-
254 netic signatures of kelvin-helmholtz vortices on saturn's magnetopause:
255 Global survey. *Journal of Geophysical Research*, *118*(1), 393-404. doi:
256 10.1029/2012JA018197
- 257 Dougherty, M., Kellock, S., Southwood, D., Balogh, A., Smith, E., Tsurutani, B.,
258 ... Cowley, S. (2004). The cassini magnetic field investigation. *Space Science*
259 *Reviews*, *114*(1-4), 331-383. doi: 10.1007/s11214-004-1432-2
- 260 Dungey, J. (1961). Interplanetary magnetic field and auroral zones. *PHYSICAL RE-*
261 *VIEW LETTERS*, *6*(2), 47-&. doi: 10.1103/PhysRevLett.6.47
- 262 Glassmeier, K.-H., Klimushkin, D., Othmer, C., & Mager, P. (2004). Ulf waves
263 at mercury: Earth, the giants, and their little brother compared. *Advances in*
264 *Space Research*, *33*(11), 1875 - 1883. Retrieved from doi: [https://doi.org/10](https://doi.org/10.1016/j.asr.2003.04.047)
265 [.1016/j.asr.2003.04.047](https://doi.org/10.1016/j.asr.2003.04.047)
- 266 Guo, R. L., Yao, Z. H., Sergis, N., Wei, Y., Mitchell, D., Roussos, E., ... Wan,
267 W. X. (2018, DEC 1). Reconnection acceleration in saturn's dayside magne-
268 todisk: A multicase study with cassini. *Astrophysical Journal Letters*, *868*(2).
269 doi: 10.3847/2041-8213/aaedab
- 270 Guo, R.-L., Yao, Z.-H., Wei, Y., Ray, L. C., Rae, I. J., Arridge, C. S., ... Dougherty,
271 M. K. (2018, AUG). Rotationally driven magnetic reconnection in saturn's
272 dayside. *Nature Astronomy*, *2*(8), 640-645. doi: 10.1038/s41550-018-0461-9
- 273 Hansen, C., Esposito, L., Stewart, A., Colwell, J., Hendrix, A., Pryor, W., ... West,
274 R. (2006, MAR 10). Enceladus' water vapor plume. *Science*, *311*(5766),
275 1422-1425. doi: 10.1126/science.1121254

- 276 Hasegawa, A., & Chen, L. (1974). Theory of magnetic pulsations. *Space Science Re-*
 277 *views*, *16*(3), 347-359. doi: 10.1007/BF00171563
- 278 Jackman, C. M., Russell, C. T., Southwood, D. J., Arridge, C. S., Achilleos, N., &
 279 Dougherty, M. K. (2007, JUN 14). Strong rapid dipolarizations in saturn's
 280 magnetotail: In situ evidence of reconnection. *Geophysical Research Letters*,
 281 *34*(11). doi: 10.1029/2007GL029764
- 282 Jackman, C. M., Thomsen, M. F., Mitchell, D. G., Sergis, N., Arridge, C. S., Fe-
 283 lici, M., . . . Dougherty, M. K. (2015, MAY). Field dipolarization in saturn's
 284 magnetotail with planetward ion flows and energetic particle flow bursts: Evi-
 285 dence of quasi-steady reconnection. *Journal of Geophysical Research*, *120*(5),
 286 3603-3617. doi: 10.1002/2015JA020995
- 287 Kanani, S. J., Arridge, C. S., Jones, G. H., Fazakerley, A. N., McAndrews, H. J.,
 288 Sergis, N., . . . Krupp, N. (2010, JUN 17). A new form of saturn's magne-
 289 topause using a dynamic pressure balance model, based on in situ, multi-
 290 instrument cassini measurements. *Journal of Geophysical Research*, *115*. doi:
 291 10.1029/2009JA014262
- 292 Keiling, A., Thaller, S., Wygant, J., & Dombeck, J. (2019, JUN). Assess-
 293 ing the global alfvén wave power flow into and out of the auroral accel-
 294 eration region during geomagnetic storms. *Science Advances*, *5*(6). doi:
 295 10.1126/sciadv.aav8411
- 296 Keiling, A., Wygant, J., Cattell, C., Mozer, F., & Russell, C. (2003, JAN 17). The
 297 global morphology of wave poynting flux: Powering the aurora. *Science*,
 298 *299*(5605), 383-386. doi: 10.1126/science.1080073
- 299 Kleindienst, G., Glassmeier, K. H., Simon, S., Dougherty, M. K., & Krupp, N.
 300 (2009). Quasiperiodic ulf-pulsations in saturn's magnetosphere. *Annales*
 301 *Geophysicae*, *27*(2), 885-894. doi: 10.5194/angeo-27-885-2009
- 302 Lee, D., & Lysak, R. (1989, DEC 1). Magnetospheric ulf wave coupling in the dipole
 303 model - the impulsive excitation. *Journal of Geophysical Research*, *94*(A12),
 304 17097-&. doi: 10.1029/JA094iA12p17097
- 305 Lepping, R., BURLAGA, L., & KLEIN, L. (1981). Surface-waves on saturns magne-
 306 topause. *Nature*, *292*(5825), 750-753. doi: 10.1038/292750a0
- 307 Lomb, N. (1976). Least-squares frequency-analysis of unequally spaced data. *Astro-*
 308 *physics and Space Science*, *39*(2), 447-462. doi: 10.1007/BF00648343
- 309 Masters, A., Achilleos, N., Bertucci, C., Dougherty, M. K., Kanani, S. J., Arridge,
 310 C. S., . . . Coates, A. J. (2009, DEC). Surface waves on saturn's dawn flank
 311 magnetopause driven by the kelvin-helmholtz instability. *PLANETARY AND*
 312 *SPACE Science*, *57*(14-15), 1769-1778. doi: 10.1016/j.pss.2009.02.010
- 313 Masters, A., Achilleos, N., Cutler, J., Coates, A., Dougherty, M., & Jones, G.
 314 (2012). Surface waves on saturn's magnetopause. *Planetary and Space Sci-*
 315 *ence*, *65*(1), 109 - 121. doi: https://doi.org/10.1016/j.pss.2012.02.007
- 316 Masters, A., Achilleos, N., Kivelson, M. G., Sergis, N., Dougherty, M. K., Thomsen,
 317 M. F., . . . Coates, A. J. (2010, JUL 27). Cassini observations of a kelvin-
 318 helmholtz vortex in saturn's outer magnetosphere. *Journal of Geophysical*
 319 *Research*, *115*. doi: 10.1029/2010JA015351
- 320 Palmaerts, B., Radioti, A., Roussos, E., Grodent, D., Gerard, J. C., Krupp, N.,
 321 & Mitchell, D. G. (2016, DEC). Pulsations of the polar cusp aurora
 322 at saturn. *Journal of Geophysical Research*, *121*(12), 11952-11963. doi:
 323 10.1002/2016JA023497
- 324 Palmaerts, B., Roussos, E., Krupp, N., Kurth, W. S., Mitchell, D. G., & Yates, J. N.
 325 (2016, JUN 1). Statistical analysis and multi-instrument overview of the quasi-
 326 periodic 1-hour pulsations in saturn's outer magnetosphere. *Icarus*, *271*, 1-18.
 327 doi: 10.1016/j.icarus.2016.01.025
- 328 Radioti, A., Grodent, D., Yao, Z. H., Gerard, J. C., Badman, S. V., Pryor, W., &
 329 Bonfond, B. (2017, DEC). Dawn auroral breakup at saturn initiated by auro-
 330 ral arcs: Uvis/cassini beginning of grand finale phase. *Journal of Geophysical*

- 331 *Research*, 122(12), 12111-12119. doi: 10.1002/2017JA024653
- 332 Radioti, A., Yao, Z., Grodent, D., Palmaerts, B., Roussos, E., Dialynas, K., ...
333 Bonfond, B. (2019, NOV 1). Auroral beads at saturn and the driving mech-
334 anism: Cassini proximal orbits. *Astrophysical Journal Letters*, 885(1). doi:
335 10.3847/2041-8213/ab4e20
- 336 Roussos, E., Krupp, N., Mitchell, D. G., Paranicas, C., Krimigis, S. M., Andri-
337 opoulou, M., ... Dougherty, M. K. (2016, JAN 1). Quasi-periodic injections of
338 relativistic electrons in saturn's outer magnetosphere. *Icarus*, 263(SI), 101-116.
339 doi: 10.1016/j.icarus.2015.04.017
- 340 Russell, C., Khurana, K., Huddleston, D., & Kivelson, M. (1998, MAY 15). Lo-
341 calized reconnection in the near jovian magnetotail. *Science*, 280(5366), 1061-
342 1064. doi: 10.1126/science.280.5366.1061
- 343 Saur, J., Janser, S., Schreiner, A., Clark, G., Mauk, B. H., Kollmann, P., ... Kot-
344 siaros, S. (2018, NOV). Wave-particle interaction of alfvén waves in jupiter's
345 magnetosphere: Auroral and magnetospheric particle acceleration. *Journal of*
346 *Geophysical Research*, 123(11), 9560-9573. doi: 10.1029/2018JA025948
- 347 Scargle, J. (1982). Studies in astronomical time-series analysis .2. statistical aspects
348 of spectral-analysis of unevenly spaced data. *Astrophysical Journal*, 263(2),
349 835-853. doi: 10.1086/160554
- 350 Slavin, J. A., Acuna, M. H., Anderson, B. J., Baker, D. N., Benna, M., Boardsen,
351 S. A., ... Zurbuchen, T. H. (2009, MAY 1). Messenger observations of mag-
352 netic reconnection in mercury's magnetosphere. *Science*, 324(5927), 606-610.
353 doi: 10.1126/science.1172011
- 354 Sun, W.-J., Slavin, J. A., Fu, S., Raines, J. M., Zong, Q.-G., Imber, S. M., ...
355 Baker, D. N. (2015, MAY 28). Messenger observations of magnetospheric
356 substorm activity in mercury's near magnetotail. *Geophysical Research Letters*,
357 42(10), 3692-3699. doi: 10.1002/2015GL064052
- 358 Vogt, M. F., Kivelson, M. G., Khurana, K. K., Joy, S. P., & Walker, R. J. (2010,
359 JUN 29). Reconnection and flows in the jovian magnetotail as inferred from
360 magnetometer observations. *Journal of Geophysical Research*, 115. doi:
361 10.1029/2009JA015098
- 362 Waite, J., Combi, M., Ip, W., Cravens, T., McNutt, R., Kasprzak, W., ... Tseng,
363 W. (2006, MAR 10). Cassini ion and neutral mass spectrometer: Ence-
364 ladus plume composition and structure. *Science*, 311(5766), 1419-1422. doi:
365 10.1126/science.1121290
- 366 Wilson, R. J., Delamere, P. A., Bagenal, F., & Masters, A. (2012). Kelvin-helmholtz
367 instability at saturn's magnetopause: Cassini ion data analysis. *Journal of*
368 *Geophysical Research*, 117(A3). doi: 10.1029/2011JA016723
- 369 Yao, Z. H., Grodent, D., Ray, L. C., Rae, I. J., Coates, A. J., Pu, Z. Y., ...
370 Dunn, W. R. (2017a). Two fundamentally different drivers of dipolariza-
371 tions at Saturn. *Journal of Geophysical Research*, 122(4), 4348-4356. doi:
372 10.1002/2017JA024060
- 373 Yao, Z., Pu, Z. Y., Rae, I. J., Radioti, A., & Kubyshkina, M. V. (2017b). Auroral
374 streamer and its role in driving wave-like pre-onset aurora. *Geoscience Letters*,
375 4(1), 8. doi: 10.1186/s40562-017-0075-6
- 376 Yao, Z. H., Radioti, A., Rae, I. J., Liu, J., Grodent, D., Ray, L. C., ... Palmaerts,
377 B. (2017c). Mechanisms of saturn's near-noon transient aurora: In situ ev-
378 idence from cassini measurements. *Geophysical Research Letters*, 44(22),
379 11,217-11,228. doi: <https://doi.org/10.1002/2017GL075108>
- 380 Yao, Z. H., Grodent, D., Kurth, W. S., Clark, G., Mauk, B. H., Kimura, T., ...
381 Levin, S. M. (2019). On the relation between jovian aurorae and the load-
382 ing/unloading of the magnetic flux: Simultaneous measurements from juno,
383 hubble space telescope, and hisaki. *Geophysical Research Letters*, 46(21),
384 11632-11641. doi: 10.1029/2019GL084201
- 385 Young, D. T., Berthelier, J. J., Blanc, M., Burch, J. L., Coates, A. J., Goldstein, R.,

- 386 ... Zinsmeyer, C. (2004, September). Cassini Plasma Spectrometer Investiga-
387 tion. *Space Science Reviews*, *114*(1-4), 1-112. doi: 10.1007/s11214-004-1406-4
388 Zhao, H., Zhou, X.-Z., Liu, Y., Zong, Q.-G., Rankin, R., Wang, Y., ... Chen, X.
389 (2019). Poleward-moving recurrent auroral arcs associated with impulse-
390 excited standing hydromagnetic waves. *Earth and Planetary Physics*, *3*(4),
391 305-313. doi: 10.26464/epp2019032
392 Zong, Q., Rankin, R., & Zhou, X. (2017, December). The interaction of ultra-low-
393 frequency pc3-5 waves with charged particles in Earth's magnetosphere. *Re-*
394 *views of Modern Plasma Physics*, *1*(1), 10. doi: 10.1007/s41614-017-0011-4
395 Zong, Q.-G., Zhou, X.-Z., Wang, Y. F., Li, X., Song, P., Baker, D. N., ... Pedersen,
396 A. (2009, OCT 10). Energetic electron response to ulf waves induced by inter-
397 planetary shocks in the outer radiation belt. *Journal of Geophysical Research*,
398 *114*. doi: 10.1029/2009JA014393

Accepted Article